Dielectric Relaxation and Its Effect on the Thermal Electric Characteristics of Insulators*

J. G. Simmons and G. W. Taylor
Department of Electrical Engineering, University of Toronto, Toronto, Canada
(Received 8 June 1971)

A theoretical study is presented of the effect of dielectric relaxation on the thermal electrical characteristics of metal-insulator-metal systems in which the electrodes make blocking contacts with the insulator. The relatively simple experimental procedures indicated by the theory provide a powerful analytical method for the study of the defect nature of the insulator and the electrode-insulator interfacial barrier parameters. Basically, the theory applies to a procedure which consists of cooling the system to low temperatures, with a constant voltage V_d applied. The temperature is then raised, at a constant rate of increase with time, with a constant voltage V_i applied such that $V_i \neq V_d$; the current-temperature characteristic obtained during the heating is the potential source of information. It is shown that during the initial stages of the heating cycle, the conduction process is bulk limited and the electrical characteristic depicted by a non-steady-state Poole–Frenkel mechanism. At the high-temperature range of the heating cycle, a steady-state electrode-limited conducting process prevails. In the intermediate-temperature range, pronounced thermally stimulated dielectric-relaxation currents (DRC) are predicted to occur. These currents exhibit pronounced maxima, and the temperatures at which they occur are related to the energies of trapping levels in the insulator and to the heights of the interfacial barriers. The area under the DRC curves is directly proportional to the charge removed from, or supplied to, the traps; a quantitative knowledge of this charge exchange permits an estimation of the trap density in the insulator.

I. INTRODUCTION

In the preceding paper[1] we discussed the effects of dielectric relaxation on the isothermal current-voltage (I-V) characteristics of metal-insulator-metal (MIM) systems in which blocking contacts existed at the metal-insulator interface. In this paper we will discuss the effect of dielectric relaxation on the thermal electrical properties of similar systems.

Here, as in the preceding paper,[1] we have chosen to study a simple insulator model, but one which may be generalized and used as a building block for more complicated structures. We have stressed the underlying physical processes, even though at times it has been at the expense of mathematical precision. Also, we have chosen to look at the process solely from the point of view of electrons rather than holes. Naturally, in some systems, holes may be the dominant agent in the process; however, it is a simple task to recast the processes discussed here in terms of holes.

In order to avoid belaboring points dealt with in the preceding paper, we have assumed that the reader has familiarized himself with the details contained therein.

II. THERMAL CHARACTERISTICS

A. System and Conventions

Figure 1(a) illustrates the MIM system under consideration. It is identical in most ways to that described in the preceding paper, to which the reader is referred for further details. However, in this paper we will be concerned more with interfacial barrier heights ϕ_1 and ϕ_2 that are not identical. (Pairs of equations relating to the properties of the two interfaces are normally identical except for the barrier heights of the interfaces. Thus, for conciseness, and where appropriate, we express this pair of equations by a single equation using the parameter ϕ; ϕ_1 and ϕ_2 are substituted for ϕ when appropriate). In Fig. 1(a), ϕ_1 and ϕ_2

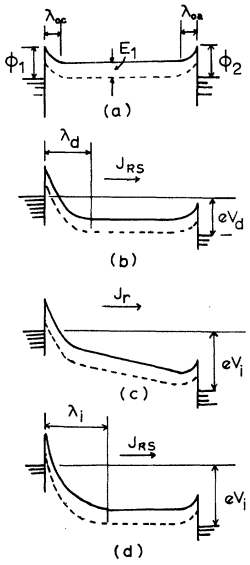

FIG. 1. Energy diagram of system: (a) under zero bias; (b) in steady-state condition with $V = V_d$; (c) immediately after voltage has been increased from V_d to V_i; (d) in steady-state condition for $V = V_i$. Arrow indicates direction of (positive) electronic current.

represent the idealized interfacial barrier heights at the left interface and right interface, respectively [see Fig. 1(a)]; hence

$$\phi_1 = \psi_1 - \chi, \quad \phi_2 = \psi_2 - \chi,$$

where ψ_1 and ψ_2 are, respectively, the work functions of the original cathode and anode and χ is the electron affinity of the insulator. In order to obtain the actual barrier height, it is necessary to include the effect of barrier lowering due to the Schottky effect. Since the barrier heights are different, the zero-bias depletion regions are different. Here, λ_{c0} and λ_{a0} are designated as the width of the depletion regions adjacent to the left and right interface, respectively (see Fig. 1).

The following conventions are used throughout this section: V_d is the applied voltage when the system is cooled to low temperature, and V_i is the applied voltage when the temperature of the system is raised. The positive direction of electronic current is from left to right in the energy diagrams (positive conventional current flows in the converse direction).

B. Effect of Temperatures on the Relaxation Process

1. Isothermal Emission of Trapped Electrons

It was shown in the preceding paper[1] that when a voltage V is applied to a MIM system having blocking contacts, the system relaxes to the steady state owing to the growth of the cathodic depletion region (CDR) [cf. Figs. 1(a) and 1(b)]. Essentially all the applied voltage V is absorbed across the CDR. This being the case, the width of the steady-state CDR, λ_c, is given by

$$\lambda_c \simeq 2(\epsilon/q^2 N_t)^{1/2}[\phi_1 - E_1 + q(V - \Delta V)]^{1/2}, \qquad (1)$$

where ϵ is the permittivity of the insulator, N_t is the trap density per cm^{-3}, E_1 is the depth of the trapping level below the bottom of the conduction band, q is the unit of electronic charge, and ΔV, which is normally a fraction of a volt and may be ignored for large V, is that portion of the voltage absorbed across the interior of the insulator and the anodic (forward-biased) Schottky barrier. The growth of the CDR is accompanied by a time-dependent relaxation current, and the dielectric relaxation process was discussed in terms of this current in the preceding paper. In particular it was shown that the dielectric relaxation time (DRT) associated with the relaxation current is given by[1]

$$t_r = 10^{-23} N_t^{1/2} e^{(E_1 - 2\beta F^{1/2})/kT}.$$

(Note that E_1 refers to the zero-field trap depth.) The term $2\beta F^{1/2}$ represents the Poole–Frenkel lowering of the barrier of the trap (assumed to be donor-type[2]), where F is the electric field at the trap (F_i if in the interior of the insulator), and β is given by

$$\beta = (q^3/4\pi\epsilon)^{1/2}.$$

For deep trapping levels and low temperatures, t_r is very large, which means that the current relaxes only slowly with time; that is, it is essentially constant. For shallow trap levels and higher temperatures, t_r is a fraction of a second, which means that the current relaxes quickly to its steady-state value.

In the preceding paper, the relaxation process was described in terms of the growth of the CDR. An alternative method of looking at the temporal decay of the relaxation process is in terms of the rate of emission of electrons from traps in the region corresponding to the CDR since the time taken to empty these traps corresponds to the relaxation time. In order to do this we proceed as follows. Let n_t' be the rate of emission of electrons from the trap level per unit volume; hence

$$n_t' = -n_t e_n, \qquad (2)$$

where n_t is the trapped-electron density at any time t in the trap level, and e_n is the emission coefficient for the trap and is given by

$$e_n = \nu e^{-(E_1 - 2\beta F^{1/2})/kT}, \qquad (3)$$

where ν ($\simeq 10^{12}$ sec^{-1}) is the attempt-to-escape frequency. The current J_r associated with this process is the relaxation current and is given by

$$J_r = -qn_t' d = qn_t e_n d, \qquad (4)$$

where d is the mean-free-drift distance of the electrons.

Now, if the system is at a constant low temperature such that e_n is constant and very small, then the density of electrons in the traps will remain essentially constant ($n_t \simeq \frac{1}{2}N_t$) during the emission process. (For example if $E_1 = 0.35$ eV and $T = 100$ °K, $e_n = 10^{-7}$; hence in 10^5 sec the traps would have been depleted of only 1% of their original charge.) Thus, for this condition, (2) can be written in the approximate form

$$n_t' = -\tfrac{1}{2}N_t e_n \qquad (5)$$

and the "constant" current density J_r associated with this charge release is, from (4) and (5), approximately

$$J_r \simeq \tfrac{1}{2}qN_t e_n d. \qquad (6)$$

Equation (6) is equivalent to the Poole–Frenkel current (see Appendix) J_{PF}:

$$J_{PF} = q\mu F_i N_c e^{-E_1/kT} e^{2\beta F_i^{1/2}/kT}, \qquad (7)$$

where μ is the electron mobility and N_c is the effective density of states in the conduction band. This conclusion regarding the relaxation current was also obtained in the preceding paper[1] using differ-

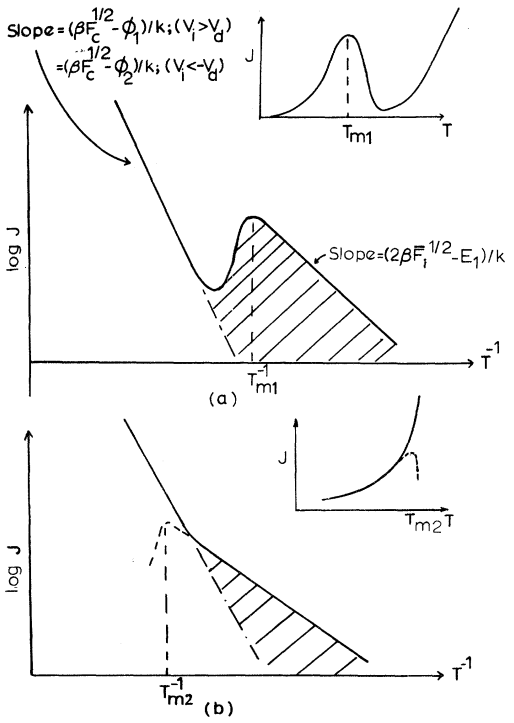

FIG. 2. $\text{Log}_{10}J$ vs T^{-1} plots for $V_i > V_d$ and $V_i < -V_d$. (Note that for $V_i < -V_d$, J is a negative current.) (a) Characteristic for good blocking contacts; inset is the corresponding linear $J-T$ characteristic. (b) Characteristic for leaky blocking contacts; inset is the corresponding resolved linear DRC $J-T$ characteristic (see text).

ent reasoning.

Consider now what happens when the temperature of the system is sufficiently high so that the emission process perturbs the occupancy of the traps. In this case, n_t and n_t' are given by

$$n_t = \tfrac{1}{2}N_t - \int_0^t n_t'\,dt \tag{8}$$

and

$$n_t' = (\tfrac{1}{2}N_t - \int_0^t n_t'\,dt)\,e_n\,. \tag{9}$$

Therefore, from (4) and (9) we have

$$J_r = q(\tfrac{1}{2}N_n - \int_0^t n_t'\,dt)e_n d\,, \tag{10}$$

which means that, at a constant temperature, J_r decays with time.

2. *Relaxation Current vs Temperature*

Suppose we cool the system to a low temperature T_0 and apply a bias V. Now let the temperature T of the system be raised at a constant rate β:

$$T = \beta t + T_0\,. \tag{11}$$

Initially $e_n \ll 1$, which means that the emission process does not significantly deplete the electrons in the trapping level; hence the current is given by (7). Thus, for a constant applied voltage the slope of a plot of $\log_{10}J$ vs $(kT)^{-1}$ yields the activation energy[2,3] $(E_1 - 2\beta F^{1/2})$ (see, for example, Fig. 2).

When e_n approaches a value of about 10^{-2} the emission process begins to significantly deplete the trapping level of its electrons, and the current is now given by (10). Because n_t decreases with increasing temperature, the rate of increase of current decreases with increasing temperature, so that at some temperature T_m the current actually *decreases* with further increase of temperature. The relaxation current ceases to flow when all the traps in the region corresponding to the steady-state CDR [see Fig. 1(d)] have been depleted of their electrons. The system is now in its steady state and hence the current flowing in the system is the steady-state current. Thus, it will be apparent that the $\log_{10}J$ vs T^{-1} (or J vs T) characteristic will manifest a (thermally stimulated) maximum, as shown, for example, in Fig. 2(a). Once the occupancy of the trapping level begins to be significantly perturbed due to the emission process, it is very quickly completely depleted of its electrons. [This will be apparent by inspection of Fig. 2(a), for example.] The portion of the $\log_{10}J$ vs T^{-1} where the current is seen to be decreasing, corresponds to the temperature range during which the traps are being significantly depleted. The point at which the characteristic begins to turn upwards again corresponds to the temperature at which the traps are empty. Since the temperature range over which trap depletion occurs is quite narrow, it follows that the time required for this process to occur is relatively short.

The solution to this problem may be approached from two different points of view. The first of these involves an analysis of the emission of charge in the CDR, and the second involves an analysis of the fields and currents in the bulk of the insulator. Using the latter approach, the exact analysis of the probelm is very complex and intractable to analytical solution. In a numerical computation one would typically begin by choosing, at a particular temperature T, and thus time t, an arbitrary value of $\lambda(T)$, the width of the cathodic space-charge region. This allows an estimation of the total charge removed from the insulator which in turn enables the calculation of the fields in the depletion region and in the interior of the insulator. Knowing the field, and hence the current, we calculate the total charge removed and compare the corresponding depletion region width to the assumed value. Through continued iteration, an accurate value of $\lambda(T)$, and hence the current, may be determined.

To avoid these complexities, we have adopted the first approach and studied the high-field CDR alone. It is seen from (4) and (10) that in order to determine the current we require to know the

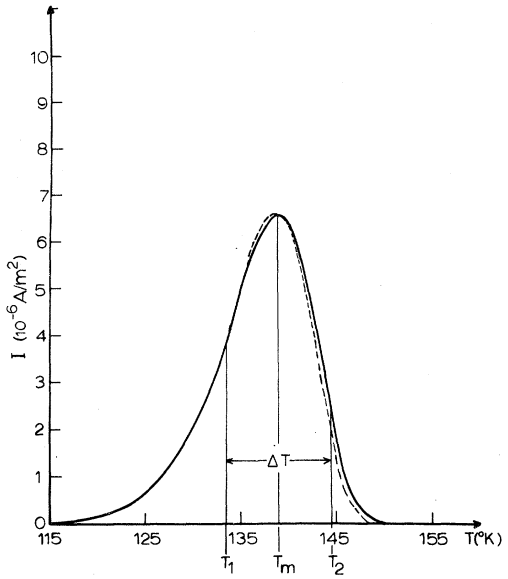

FIG. 3. Theoretical DRC characteristic for a discrete trapping level, obtained using (a) expression (15) (solid line) and (b) a numerical calculation of the DRC during the relaxation of the CDR (dotted line).

mean-free-drift distance, which in this case is equal to $\lambda(T)$. Since the variation in temperature of this parameter is unknown, in order to facilitate the discussion we use an approximate constant for λ, $\bar{\lambda}$, which is chosen in the following manner. For very low temperatures this approximation will yield slightly excessive values of current, but the current in this temperature range yields little information in any event because its magnitude is so small. At temperatures just above that (T_m) corresponding to the maximum in current, $\lambda(T)$ has almost attained its steady-state value λ_c and the current is dominated by the exponential variation in the trap occupancy. Also, it can be shown that the trap occupancy has been reduced to e^{-1} of its original value at $T = T_m$. Thus, since the width of the depletion region is proportional to the charge removed from the traps, we choose $\bar{\lambda} = \lambda_c[(e-1)/e]$ as a representative value of $\lambda(T)$ for the entire temperature range. From similar arguments to these it also follows that the field $F(T)$ at the trapping center during the emission process may be represented by an average value $\bar{F}_i = F_{i0}[e/(e-1)]$, where F_{i0} is the field at the edge of the CDR at the start of the heating process; that is, $F_{i0} = V_i/L$, where L is the length of the insulator. The fact that these assumptions are justified is well illustrated by the dielectric-relaxation-current-(DRC)-versus-T curves in Fig. 3, which shows the solution obtained using the first approach and the above approximations (solid line), and that obtained using the second approach (dotted line), with no approximations.

The temperature T_m at which the maximum in the DRC characteristic occurs is obtained as follows. From (4), assuming that d is relatively constant near T_m,

$$\frac{1}{q}\frac{dJ}{dT} \simeq n_t' \frac{dt}{dT} e_n \bar{\lambda} + \frac{1}{kT^2}(E_1 - 2\beta\bar{F}_i^{1/2}) n_t e_n \bar{\lambda} = 0 . \tag{12}$$

Substituting for n' from (2), and since $dT/dt = B$ from (10), we have

$$\frac{B(E_1 - 2\beta\bar{F}_i^{1/2})}{kT_m^2} = e_n = \nu \exp\left[-\left(\frac{E_1 - 2\beta\bar{F}_i^{1/2}}{kT_m}\right)\right]. \tag{13}$$

Since all the parameters in (13) are known, $(E_1 - 2\beta\bar{F}_i^{1/2})$ and hence E_1 can be determined; note that the former energy is the activation energy[2,3] of the conduction process preceding the dielectric relaxation current (DRC) peak [see (7)]. Equation (13) is rather inconvenient since $(E_1 - 2\beta\bar{F}_i^{1/2})$ is expressed in transcendental form. However, it can be shown[4] that (13) can be expressed in the approximate analytical form

$$E_1 - 2\beta\bar{F}_i^{1/2} = T[1.92\times10^{-4}\log_{10}(\nu/B) + 3.2\times10^{-4}] - 0.0155 \text{ eV} . \tag{14}$$

It will be noted that the temperature at which the peak occurs is independent of the width of the CDR. However, as we shall see shortly, the area under the DRC peak is directly proportional to the charge in the CDR due to the applied voltage.

The electrons responsible for the relaxation current are released from traps located at the edge of the CDR (see Sec. II B 1). Thus, retrapping of electrons in the CDR is negligible, which means that first-order kinetics[4] are applicable. The J-T characteristic under these conditions is given by[4,5] (see Fig. 3)

$$J(T) = \frac{q\bar{\lambda}}{2} N_t e_n \exp\left[-\frac{e_n kT^2}{E_1 - 2\beta\bar{F}_i^{1/2} + kT}\right] . \tag{15}$$

If the DRC peak arises from a discrete trapping level, its half-width ΔT is given by[4]

$$\Delta T = 2kT_m^2/(E_1 - 2\beta\bar{F}_i^{1/2}) , \tag{16}$$

where $\Delta T = (T_a - T_b)$ and T_a and T_b $(T_a > T_b)$ are the temperatures at which the current is half the maximum current, as shown in Fig. 3. Otherwise, the curve is due to a distribution of traps; this case is treated elsewhere.[4]

3. *Charge Released during Relaxation Process*

Let Q_r be the increase in space charge per unit area of the CDR and hence the charge removed from the insulator as the system relaxes to the steady state. Assuming that the insulator thickness is much greater than the CDR, then a charge of approximately Q_r circulates in the external circuit.[6]

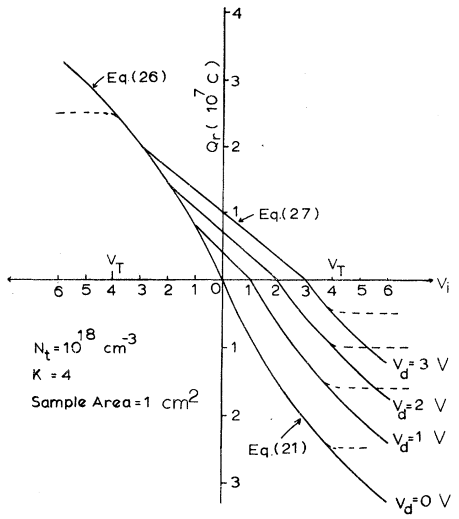

FIG. 4. Family of Q_r vs V_d curves with V_d as a parameter.

Since essentially all the charge Q_r is released from the traps in the temperature range (T_1 to T_2) when the DRC peak is apparent on a linear J-T plot (see Fig. 4),[7] the area A under the DRC peak can be related to Q_r as follows:

$$A = \int_{T_1}^{T_2} J\,dT\ , \tag{17}$$

and from (11)

$$A = B\int_{t_1}^{t_2} J\,dt = BQ_r\ . \tag{18}$$

In (18), t_1 and t_2 are the times corresponding to T_1 and T_2, respectively. Thus, the number of released carriers and the depth of the trap may be obtained from the DRC peak. It will be apparent from (1) and (15) that the greater is V, the greater is the charge released from the traps.

4. Steady-State Characteristic and Effect of Leaky Contacts

The steady-state J-T characteristic for a particular applied voltage V is obtained by applying the voltage at a sufficiently high temperature such that the system is in the steady state. It will be apparent that if the sample is now cooled slowly to low temperatures with the voltage still applied, it will be in its steady-state condition at the low temperature [see Fig. 2(b)]. The J-V-T relationship under this condition is given by the Richardson–Schottky expression

$$J = J_0 e^{-\phi/kT} e^{\beta F_c^{1/2}/kT}\ \mathrm{Am}^{-2} \tag{19}$$

where J_0 is given[8] by

$$J_0 = 1.2\times 10^6 T^2\ .$$

In the above expression ϕ and F_c are, respectively, the height of the interfacial barrier and the field at the cathode-insulator interface. For the steady-state condition considered here, F_c is given by

$$F_c \simeq (N_t/\epsilon)^{1/2}[\phi - E_1 + q(V - \Delta V)]^{1/2}\ . \tag{20}$$

If the system temperature is now raised with the voltage V still applied, a DRC will not be observed, since the system is in the steady state; that is, the conduction process described by (19) will prevail at all temperatures. The activation energy of this process is $(\phi - \beta F_c^{1/2})$ and is higher than that associated with the non-steady-state process described by (7). A procedure for determining whether or not the system is in its steady-state condition is to observe the J-T characteristic for *both* decreasing and increasing temperature; the two characteristics should be identical.

A knowledge of the J-V characteristic for the steady state is important if the electrodes do not make particularly good blocking contacts to the insulator, since the background steady-state current may be of the same order of magnitude as the DRC at the maximum. When this is the case a DRC peak may not actually be manifest, but rather a change in slope in the $\log_{10}J$ vs T^{-1} characteristic. (Of course, a change in slope does not necessarily imply a non-steady-state situation; whether or not the process is steady state or otherwise is determined by the test procedure described in the previous paragraph.) A particular example of this case is shown in Fig. 2(b) where the non-steady-state characteristic, of slope $E_1 - 2\beta\bar{F}_i^{1/2}$, merges with the steady-state characteristic, which exhibits a slope $\phi - \beta F_c^{1/2}$. This situation arises when the rate of rise of temperature is such that the temperature corresponding to the DRC maximum is higher than that at which the steady-state current becomes comparable to the relaxation current [see dotted curve in Fig. 2(b)]. To resolve the DRC peak it is necessary to reduce the rate of rise of temperature, B.

Up to this point we have discussed the relaxation currents in general terms. The rest of the paper is devoted to a study of relaxation currents associated with various conditions of voltage bias, each case having to be discussed on its own merits.

C. Case $V_i > V_d$

1. J-T Characteristic

Consider the case when V_i (voltage applied for increasing temperature) is greater than V_d (voltage applied for decreasing temperatures). Figure 1(b) illustrates the energy diagram for the system in the steady state at low temperatures with a voltage bias V_d applied; the steady-state current for this case flows in the positive direction as indicated by the arrow in the figure. Figure 1(c) is the energy

diagram for the system at the start of the heating cycle at low temperatures after the applied voltage has been increased from V_d to V_i. Figure 1(d) is the energy diagram for the system in the steady state with a voltage V_i applied. It will be apparent that, since in the interior of the insulator the slope of the conduction band in Fig. 1(c) is in the same direction as for the original bias V_d, the relaxation current flows in the same (positive) direction as the steady-state current for the original bias. (This fact could also have been deduced from the fact that the CDR grows in size during the relaxation period.) Figures 2(a) and 2(b) represent the two possible types of $\log_{10}J$ vs T^{-1} curves that are generated during the relaxation process. Figure 2(a) corresponds to a system having good blocking contacts, and Fig. 2(b) to a system having leaky contacts. In both these curves the linear region of the low-temperature J-T characteristic is given by (7); hence the slope of the curves is given by[2,3] $(2\beta\bar{F}_i^{1/2} - E_1)/k$. The linear portion at the higher temperature is the steady-state J-T characteristic (19); thus the slope of this portion is $(\beta F_c^{1/2} - \phi_1)/k$. The relaxation current is actually the hatched section shown on the curves; that is, it is the difference between the observed non-steady-state curve and the extended portion (chain-dotted) of the steady-state curve. In the case of Fig. 2(a) the DRC peak is clearly manifested on either the $\log_{10}J - T^{-1}$ plot or a linear J-T plot [see insert in Fig. 2(a)]. In the latter case [Fig. 2(b)] the area under the curve is equal to βQ_r [see (18)]. In the second case the DRC peak is not manifested in the $\log_{10}J - T^{-1}$ plot. To resolve the peak the rate of rise of temperature must be decreased (see Sec. IIC 4).

2. Q_r vs V_i

Designating λ_{ci} and λ_{cd} as the width of the steady-state cathodic depletion regions for applied voltages V_i and V_d, respectively, the charge Q_r released during the relaxation process is

$$Q_r = q(\tfrac{1}{2}N_t)(\lambda_{ci} - \lambda_{cd})$$

$$= (\epsilon N_t)^{1/2}[(\phi_1 - E_1 + qV_i)^{1/2} - (\phi_1 - E_1 + qV_d)^{1/2}]\,. \quad (21)$$

In Fig. 4 the family of curves in the lower part of the diagram represent Q_r as a function of V_i with V_d as a parameter. Hence, using various fixed values of V_d, the family of Q_r-vs-V_i curves are generated. It will be noted that Q_r is always zero for $V_i = V_d$, and this is because the system is in steady state during the cooling *and* heating cycles (see Sec. IIC 4). Also, the greater the difference $V_i - V_d$, the greater is Q_r.

In Fig. 4 at high values of V_i, Q_r is shown to saturate. The reason for this is an electrode-limited–to–bulk-limited transition[9] in the conduction process as follows. Under steady-state conditions the greater the value of V_i, the greater is the field at the cathode-insulator interface, which in turn means that the thickness of the potential barrier at the interface, Δs (that is, the distance from the interface to the bottom of the conduction band measured at the cathode Fermi level) also decreases. When the barrier thickness is approximately 100 Å or less, electrons tunnel from the cathode into the insulator; thus the cathode contact is no longer a blocking contact. The J-V characteristic of the barrier for this process is given by[9]

$$J = \frac{1.22\times10^{-11}N_t(V+\psi_m-\psi_i)}{2\phi K^3} \times \exp\left[-\frac{3.65\times10^{10}(2K\phi_1^3)^{1/2}}{N_t(V+\psi_m-\psi_i)^{1/2}}\right] \text{A cm}^{-2}, \quad (22)$$

where K is the insulator dielectric constant, and ϕ_1, ψ_m and ψ_i are expressed in electron volts, and N_t in traps cm^{-3}. From a comparison of (7) and (22) it will be apparent that the resistance of the barrier decreases much more rapidly with increasing voltage bias than that of the bulk, although initially the barrier resistance is much higher than that of the bulk. Hence, at some particular voltage V_T, the transition voltage, the resistance of the contact drops below that of the bulk. Thereafter, practically all of the voltage in excess of V_T is absorbed across the bulk and the remaining fraction across the barrier, just sufficient to ensure current continuity throughout the system. Therefore, for $V_i > V_T$ the depletion region essentially ceases to grow, or, in other words, Q_r saturates. V_T may be evaluated approximately in the following manner. The potential barrier (as viewed from the cathodic Fermi level) may be considered to be triangular and hence, throughout its width, the field is considered constant and equal to its interfacial value F_0. Thus Δs is given by

$$\Delta s = \phi_1/qF_c\,, \quad (23)$$

where F_c is given by (20) with V replaced by V_i:

$$F_c \simeq 1.4\times10^{-3}N_t^{1/2}[(V_i+\phi_1-E_1)/K]^{1/2}\ \text{V cm}^{-1}\,. \quad (24)$$

Assuming $\Delta s \simeq 50$ Å when $V_i = V_T$, we have from (23) and (24)

$$V_T \simeq 2\times10^{18}(\phi_1^2K/N_t) + E_1 - \phi_1\,. \quad (25)$$

In (24) and (25), ϕ_1 and E_1 are expressed in electron volts and N_t in cm^{-3}. Thus, for $\phi = 1$ eV, $E_1 = 0.5$ eV, $K = 5$, and $N_t = 10^{18}$ cm^{-3}, $V_t = 9.5$ V. Normally one would calculate N_t knowing V_T. This method should give the correct order of magnitude for N_t, which should, of course, correspond to that obtained from the DRC curve.

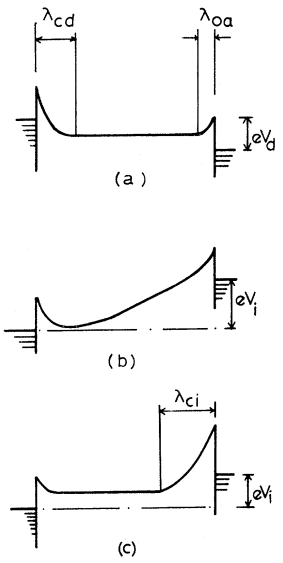

FIG. 5. Energy diagram of system: (a) in steady-state condition with a bias $V_d > 0$; (b) immediately after a voltage V_i ($< -V_d$) is applied; (c) in steady-state condition for $V = V_i$. Arrows indicate direction of electronic current flow.

D. Case $V_i < -V_d$

1. J-T Characteristics

Figure 5(a) illustrates the energy diagram for the system in its steady-state condition at low temperatures with a voltage bias V_d applied [cf. Fig. 1(b)]. Figure 5(b) is the energy diagram for the system at the start of the heating cycle after the voltage has been decreased to V_i. Figure 5(c) is the energy diagram for the system in the steady state with a voltage V_i applied. For $V_i < -V_d$ the width of the new cathode[10] depletion region is greater than that of the original CDR. Hence, the charge Q_r released during the growth of the former is more than sufficient to neutralize the excess positive charge Q_c accumulated in the latter (i.e., it reduces it to approximately its zero-bias value) due to the applied voltage V_d. What this means is that the system relaxes directly to its steady-state condition rather than the quasi-steady-state[1] (see Sec. II F 1). At the beginning of the heating cycle, since the slope of the conduction band in the interior of the insulator [Fig. 5(b)] is in the opposite direction to that for the original bias V_d [Fig. 5(a)], the relaxation current flows in the opposite (negative) direction to that of the original steady-state current. Also, for increasing temperatures, when the system is in the steady state, the activation energy reflects that of the right barrier[10] (i.e., $\phi_2 - \beta F_c^{1/2}$). This is to be contrasted to the analogous case for decreasing temperatures, which yields the activation energy of the left barrier (i.e., $\phi_1 - \beta F_c^{1/2}$). Note, however, that the remarks pertaining to the $\log_{10} J$ vs T^{-1} and J vs T (see Fig. 2) for blocking and leaky contacts for the case $V_i > V_d$, discussed previously in Sec. II D 1, also apply to the case at hand, and the reader is referred back to that section for the details.

2. Q_r vs V_i

The charge Q_r released during the relaxation process is given by[1]

$$Q_r = q(\tfrac{1}{2}N_t)(\lambda_{ci} - \lambda_{a0})$$

$$\simeq (\epsilon N_t)^{1/2}[(\phi_2 - E_1 + qV_i)^{1/2} - (\phi_2 - E_1)^{1/2}], \qquad (26)$$

where λ_{ci} is the steady-state width of the new cathodic[10] depletion region. The nonlinear curve in the second quadrant of Fig. 4 illustrates the Q_r-V_i relationship (26), which is independent of V_d. Merging with this curve are the linear portions (to be discussed later) of the various members of the Q_r-V_i-V_d family, the points of contact occurring at values of $|V_i|$ equal to the characteristic values of V_d for the various members. The saturated portion of the curves beyond the nonlinear regions corresponding to (26) has as its origin the same process causing the saturation of the curves in the lower half of Fig. 4 (see Sec. II C 2 for details).

E. Case $-V_d < V_i < V_d$

1. Quasi-Equilibrium-State

The dotted outline in Fig. 6(a) [cf. Figs. 1(b) and 5(a)] represents the energy diagram of the system in its steady-state condition at low temperature with a voltage bias V_d applied. The

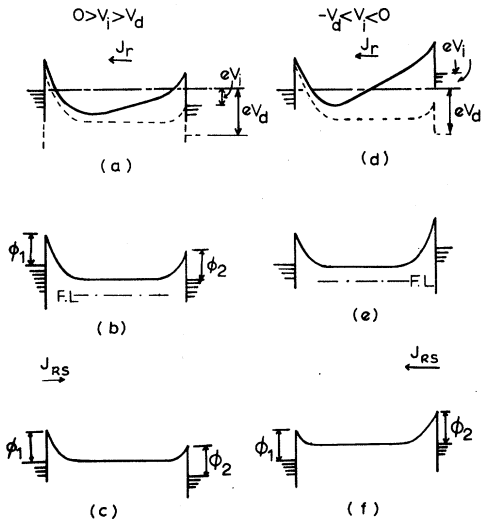

FIG. 6. Energy diagram for system: (a) immediately after voltage has been reduced from V_d to V_i (> 0); (b) in quasi-steady-state for $V = V_i$; (c) in steady-state condition for $V = V_i$. (d), (e), and (f) correspond to (a), (b), and (c), respectively, for $(-V_d) < V_i < 0$.

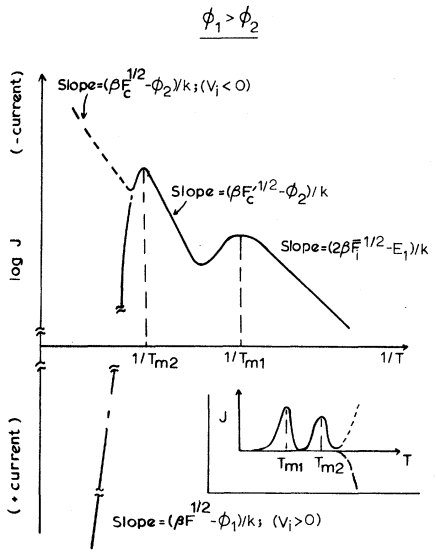

FIG. 7. $\text{Log}_{10}J$ vs T^{-1} characteristic for relaxation to quasi-steady-state and quasi-steady-state to steady state for $\phi_1 > \phi_2$. See text for further details.

charge Q_c removed from the insulator due to the application of the bias V_d is given by

$$Q_c = q(\tfrac{1}{2}N_t)(\lambda_{cd} - \lambda_{c0})$$

$$= (\epsilon N_t)^{1/2}[(\phi_1 - E_1 + qV_d)^{1/2} - (\phi_1 - E_1)^{1/2}] .$$

The solid outline in Fig. 6(a) illustrates the energy diagram for the system after the voltage has been decreased to V_i (> 0) and at the start of the heating cycle. Assuming that good blocking contacts exist on the insulator, the system relaxes to the quasi-steady-state,[1] as depicted by the energy diagram in Fig. 6(b), when its temperature reaches the relaxation temperature T_m [see (13)] for the system. Figures 6(d) and 6(e) correspond to Figs. 6(a) and 6(b), respectively, for the case $(V_i < 0)$, and remarks concerning either of the situations corresponding to Figs. 6(a) and 6(b) also pertain to the situation corresponding to Figs. 6(d) and 6(e), respectively, unless specifically stated otherwise. Figures 6(g) and 6(f) indicate the steady-state conditions for the two cases.

It will be apparent from a comparison of Figs. 6(a) and 6(b) that in relaxing to the quasi-steady-state the original anodic depletion region (ADR) increases in size. The charge released from this depletion region during the relaxation process is captured in the original CDR, with the result that this region decreases in size during the relaxation process. Hence, the electronic relaxation current flows in the opposite (negative) direction to that for the original bias V_d. Note that for the particular case when $V_i > 0$ [Fig. 6(b)] the electronic relaxation current flows from the positively biased electrode to the negatively biased electrode, hence the conventional current in the external circuit flows from the negative to the positive terminals of the battery. At temperatures at which the rate of emission of electrons from the traps does not significantly perturb the occupancy of the level, the J-T relationship is given by (7). Hence, the activation energy of the conduction process prior to the DRC peak is $(E_1 - 2\beta F_i^{1/2})$, as shown in Fig. 7.

The temperature T_{m1} at which the DRC maximum occurs as the system relaxes to the quasi-steady-state is given by (13) with T_m replaced by T_{m1}. This peak is illustrated schematically by the peak occurring at the lower temperature (T_{m1}) in the $\log_{10}J$-T^{-1} plot in the upper half of Fig. 7 and in the linear J-T plot shown in the inset in the same figure.[11] The remarks in Sec. II C 2 concerning leaky contacts and the necessary procedure for resolving the DRC peak also apply here when the contacts are leaky.

Let us assume an amount of charge ΔQ is transferred from the original anodic[10] depletion region to the opposite depletion region during the relaxation process. Therefore, provided both depletion regions are small compared to the length of the insulator, a charge $Q_r \simeq \Delta Q$ circulates the external circuit. ΔQ and hence Q_r are given by

$$\Delta Q = Q_r = \frac{(q\epsilon N_t)^{1/2}}{2} \frac{(V_d - V_i)}{(V_d + \Delta\psi_1)^{1/2} + \Delta\psi_2^{1/2}} , \quad (27)$$

where $\Delta\psi_1 = (\psi_{m1} - \psi_i)/q$ and $\Delta\psi_2 = (\psi_{m2} - \psi_i)/q$. Hence, for the particular voltage range under consideration, the area under the DRC peak, which is linear in Q_r [see (18)] is linear in V_i. The linear regions of the family of curves in the upper half of Fig. 4 represent Q_r as a function of V_i with V_d as a parameter. In this figure positive values of V_i mean that the sample is biased with the same voltage polarity as when its temperature was lowered. The zero value of V_i means that the sample is short circuited during heating, and negative values indicate an applied bias of the opposite polarity [see Fig. 6(d)] to that during cooling. As mentioned in Sec. II E, $V_d = V_i$ on all the curves simply means that the system is in the steady state as the temperature is raised; hence $Q_r = 0$. The nonlinear portions of the curves occurring at the higher negative values of V_i were discussed in Sec. II D.

2. *Steady-State Relaxation Process*

In order for the system to relax completely to the steady state from the quasi-steady-state, an amount of negative charge equal to Q_c is required to be injected from the electrodes into the insulator.[1] If the electrodes made good blocking contacts to the insulator, and if the heating process

were interrupted at a temperature just above that at which the system relaxes to the quasi-steady-state, the system would require a long period of time to relax to the steady state. In fact, if $\int J\,dt \ll Q_c$, then the flow of electrons across the barriers does not significantly perturb the excess positive charge Q_c stored in the insulator, and the quasi-steady-state prevails indefinitely. If the barriers were identical at all times during the relaxation process, the relaxation current would consist of two equal and opposite electronic currents flowing across both interfaces into the insulator; hence, no current would circulate the external circuit. Generally speaking, however, the two barriers will not be equal, and, this being the case, the electronic relaxation charge will flow predominantly across the lower of the two barriers into the insulator. (Note that since the relaxation current is a non-steady-state current, the direction of flow of the net relaxation current is not determined by the polarity of bias of the system.) Hence, a conventional current will flow in the external circuit away from the electrode at which the lower interfacial barrier exists, and if the relaxation current does not significantly perturb the excess charge stored in the insulator, it will appear to be essentially constant during the normal course of a dc measurement. Naturally, the lower interfacial barrier may exist at the surface of either the negatively or positively biased electrode, and, as we shall see, the J-V characteristic is dependent on which of the two situations prevail. We will treat the two cases separately.

a. Lower barrier at original anode ($\phi_2 < \phi_1$). For this case the current in the external circuit flows in the same direction as that of the current flow during the relaxation to the quasi-steady-state. During the initial stages of heating, the relaxation current does not significantly perturb the stored excess charge; hence, the relaxation current will be observed to increase with increasing temperature according to

$$J = J_0\, e^{-(\phi_2 - \beta F_2'^{1/2})/kT}\,. \tag{28}$$

It should be noted that, since the system is not in the steady state, the field F_2' at the interface is not given by (20) but rather by

$$F_2' = (N_t/\epsilon)^{1/2}(\phi_2 - E_1)^{1/2} + \Delta Q/\epsilon\,.$$

Since the activation energy $(\phi_2 - \beta F_2'^{1/2})$ of this conduction process is necessarily greater than that $(E_1 - 2\,\beta F_i^{1/2})$ of the Poole–Frenkel process (7), the rate of increase of the observed current [on a $\log_{10}J$ vs T plot (see Fig. 7)] after the appearance of the lower-temperature DRC peak ($T > T_{m1}$) will be greater than that of the current before the appearance of the peak ($T < T_{m1}$), as shown in Fig. 7. With continued heating, a temperature, say T_{m2}, will be approached when the relaxation current begins to perturb the excess stored charge in the insulator. As a result, the field and hence the Schottky-barrier lowering at the original anode-insulator interface (across which the relaxation current flows) decreases. This means that the relaxation current ceases to increase as rapidly as given by (28). When the stored excess charge has been completely neutralized, the relaxation current drops to zero; hence, a second DRC peak is generated in the $\log_{10}J$ vs T_1 characteristic (see Fig. 7).

After the relaxation current ceases to flow, only the steady-state current, which is injected into the insulator from the cathode, flows in the circuit. If $V_i < 0$,[10] then the current flows in the same (negative) direction as that of the relaxation currents, as indicated by the dotted line in the upper-half[11] (negative J) of Fig. 7. Hence, the J-T characteristic is given by

$$J = J_0 e^{-(\phi_2 - \beta F_c^{1/2})/kT}\,, \tag{29}$$

and the activation energy of the process is that of the barrier height of the original anode, $\phi_2 - \beta F_c^{1/2}$.

On the other hand, if $V_i > 0$, then the current flows in the opposite (positive) direction to that of the current associated with the two relaxation processes. Therefore, the current in the external circuit reverses direction when the steady-state current takes over from the non-steady-state current, as indicated by the chain-dotted line in the lower- (positive J) half of Fig. 7. Furthermore, the activation energy associated with the steady-state current

$$J = J_0 e^{-(\phi_1 - \beta F_c^{1/2})/kT}\,, \tag{30}$$

is that of the barrier height of the original cathode, $\phi_1 - \beta F_c^{1/2}$. In (29) and (30), since the system is in its steady state, F_c is given by (20). The inset in the lower-half of Fig. 7 illustrates the linear J vs T characteristic for the case in hand.

b. Lower barrier at original cathode ($\phi_1 < \phi_2$). For this case, during the relaxation process to the steady state, the current flows in the opposite (positive) direction[11] to that of the current flow associated with the relaxation to the quasi-steady-state as shown in Fig. 8. Hence, there is a reversal in the direction of the current flow as the second relaxation process takes over from the first. During the initial stages of heating, assuming that the relaxation current does not significantly perturb the stored excess charge, the J-T characteristic is given by

$$J = J_0 e^{-(\phi_1 - \beta F_1'^{1/2})/kT}\,, \tag{31}$$

where

$$F_1' = (N_t/\epsilon)^{1/2}(\phi_1 - E_1 + eV_d)^{1/2} - \Delta Q/\epsilon\,.$$

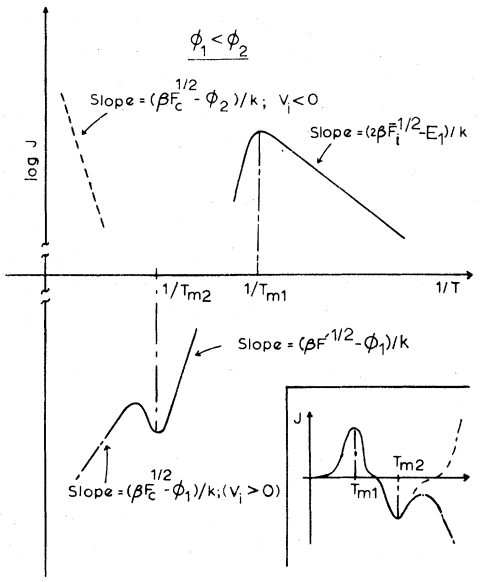

FIG. 8. $\text{Log}_{10} J$ vs T^{-1} characteristic for relaxation from the non-steady-state to the quasi-steady-state and from the quasi-steady-state to the steady state for $\phi_2 > \phi_1$. See text for further details.

When the current significantly perturbs the stored charge, the rate of increase of current with temperature decreases. Finally, with further increase in T, the current declines, resulting in a DRC peak at, say, T_{m2}. Thereafter, only the steady-state (Richardson–Schottky) current flows in the system.

If $V_i > 0$, the steady-state current flows in the same (positive) direction as that of the current flow associated with the second relaxation process, as indicated by the dotted line in the upper-half of Fig. 8, and the J-T characteristic is given by

$$J = J_0 e^{-(\phi_1 - \beta F_c^{1/2})/kT} . \tag{32}$$

When $V_i < 0$, the steady-state current flows in the opposite direction to that of the current flow associated with the second relaxation process, as indicated by the dotted curve extending from the upper- to the lower-half of Fig. 8. The J-T characteristic for this case is given by

$$J = J_0 e^{-(\phi_2 - \beta F_c^{1/2})/kT} . \tag{33}$$

3. Distinguishing between Electrode and Bulk Relaxation Processes

The quasi-steady-state to steady-state relaxation process is an electrode effect, while the relaxation processes to the quasi-steady-state are associated with bulk properties. In the latter case, if more than one trapping level exists in the insulator, it is possible to have more than one DRC peak appearing in the J-T characteristic, which would appear to complicate the matter further still. This being the case, it would appear that it would be difficult to distinguish whether a DRC peak owed its origin to the electrode effect or the bulk effect. In actual fact, the two may be readily distinguished. This is because, within the terms of our convention, relaxation currents associated with the insulator bulk always flow in the negative direction when $V_i < V_d$; that is, they are not dependent on which electrode is chosen as the cathode. However, the direction of the relaxation current associated with the electrodes is dependent on which of the electrodes is chosen as cathode. Thus, let us perform two experiments that are identical in every respect, except that between experiments the positions of the sample electrodes are interchanged. The directions of current flow associated with the bulk relaxation processes will be the same for both experiments, but will be the opposite for those of current flow associated with electrode relaxation processes.

III. CONCLUDING REMARKS

The thermal properties of the electrical characteristics of defect insulators having Schottky barriers have been presented in detail. It has been shown that measurements suggested by the theory presented here, together with those suggested in the previous paper, provide powerful techniques for characterizing the active trapping centers in the insulator. In a way, the results obtained by the electrical DRC technique presented here provide more valuable information than the optical TSC technique.[12] The former technique characterizes the trapping centers around the system Fermi level, whereas the latter tends to provide information on traps positioned below the system Fermi level. Certainly, the electrical DRC technique is a good deal easier to implement and analyze than the optical TSC technique.[12]

We have concerned ourselves with what is, in essence, a single-trapping-level system. If more than one trapping level is active in forming the depletion regions adjacent to the contacts, it will be apparent that an additional DRC peak may be manifest for every trap involved, provided that they are competitive. The analyses of any additional peaks proceed along the lines shown here for the single-trapping level. Distributed trapping levels are a rather special situation; this case is currently being studied in detail.[4]

APPENDIX

Since d is the mean-free-drift distance of the electron in the insulator, then it may be expressed as follows:

$$d = v_d \tau = \mu F_i \tau, \tag{A1}$$

where v_d is the drift velocity of the electron. τ is the electron lifetime, which is given by

$$\tau = (v_{\text{th}}\sigma_n^{\frac{1}{2}}N_t)^{-1}, \tag{A2}$$

where v_{th} is the thermal velocity of the electron, and σ_n is the electron-capture cross section. Since the attempt-to-escape frequency ν is given by

$$\nu = v_{\text{th}}\sigma_n N_c,$$

(3) may be written

$$e_n = v_{\text{th}}\sigma_n N_c e^{-(E_1 - 2\beta F_i^{1/2})/kT}. \tag{A3}$$

Substituting (A1) and (A2) into (6) yields (7).

Clearly, (6) has been obtained from (7) on the assumption that the free electrons are in thermal equilibrium with the lattice. This assumption may be an oversimplification at high fields if the electrons are not thermalized. In the latter event, a more appropriate treatment can be expected to alter the pre-exponential factor by a numerical factor probably not far removed from unity. Thus, for this reason, and because any treatment at this point in time involving hot electrons in amorphous insulators is liable to involve assumptions that in themselves would introduce relatively large numerical errors, it seems appropriate to use (7). Finally, the functional form of the electrical characteristics is essentially determined by the exponential factor, the pre-exponential factor playing only a relatively minor role.

---

*Work supported in part by Defense Research Board and National Research Council of Canada under Grant No. A7124.

[1]J. G. Simmons and G. W. Taylor, preceding paper, Phys. Rev. 6, 4793 (1972).

[2]If the traps are acceptor-type they will not experience the Poole–Frenkel effect [see J. G. Simmons, Phys. Chem. Solids 32, 258 (1971); 32, 2591 (1971)].

[3]If the trapping density is high and the DRC peak occurs at relatively low temperature, the activation energy of the conduction process prior to the occurrence of the DRC peak may be dominated by a tunnel hopping process. This process is relatively temperature insensitive; hence, its associated activation energy is much smaller than that $(E_1 - 2\beta F^{1/2})$ associated with the Poole–Frenkel conduction process.

[4]J. G. Simmons and G. W. Taylor, Phys. Rev. B 5, 1619 (1972).

[5]In the original expression derived in Ref. 4, L is used in place of $\bar{\lambda}$. This is because in that paper traps through out the insulator participate in the DRC process, whereas in the present only those in a distance $\bar{\lambda}$ participate.

[6]If λ_c were of the same order of magnitude as L, then the charge that circulated in the external circuit, Q_e, would be $Q_e \simeq Q_r(L - \lambda_c)/L$.

[7]The DRC is present all the time but does not become apparent on a *linear J-T* plot until temperatures close to T_m.

[8]J. G. Simmons, Phys. Rev. Letters 15, 967 (1965).

[9]J. G. Simmons, Phys. Rev. 166, 912 (1968).

[10]Note that for $V_i < 0$ the original anode (right electrode) is now the cathode and the original cathode is now the anode.

[11]Note that in Fig. 7, for the sake of clarity, negative currents are plotted in the upper-half of the figure and positive currents in the lower-half.

[12]R. H. Bube, *Photoconductivity in Solids* (Wiley, New York, 1960).